LIMNOLOGY
and
OCEANOGRAPHY: METHODS

ASLO

Limnol. Oceanogr.: Methods 15, 2017, 417–428

doi: 10.1002/lom3.10181

Extraction efficiency and quantification of dissolved metabolites in targeted marine metabolomics

Winifred M. Johnson [1]*, **Melissa C. Kido Soule**,[2] **Elizabeth B. Kujawinski** [2]

[1]MIT/WHOI Joint Program in Oceanography/Applied Ocean Sciences and Engineering, Department of Marine Chemistry & Geochemistry, Woods Hole Oceanographic Institution, Woods Hole, Massachusetts

[2]Department of Marine Chemistry & Geochemistry, Woods Hole Oceanographic Institution, Woods Hole, Massachusetts

Abstract

The field of metabolomics seeks to characterize the suite of small molecules that comprise the end-products of cellular regulation. Metabolomics has been used in biomedical applications as well as environmental studies that explore ecological and biogeochemical questions. We have developed a targeted metabolomics method using electrospray ionization–liquid chromatography tandem mass spectrometry to analyze metabolites dissolved in seawater. Preparation of samples from the marine environment presents challenges because dilute metabolites must be concentrated and desalted. We present the extraction efficiencies of 89 metabolites in our targeted method using solid phase extraction (SPE). In addition, we calculate the limits of detection and quantification for the metabolites in the method and compare the instrument response factors in five different matrices ranging from deionized water to spent medium from cultured marine microbes. High background organic matter content reduces the instrument response factor for only a small group of metabolites, yet enhances the extraction efficiency for other metabolites on the SPE cartridge used here, a modified styrene-divinylbenzene polymer called PPL. Aromatic or larger uncharged compounds, in particular, are reproducibly well retained on the PPL polymer. This method is suitable for the detection of dissolved metabolites in marine samples, with limits of detection ranging from < 1 pM to ~ 2 nM dependent on the dual impacts of seawater matrix on extraction efficiency and on instrument response factors.

Metabolomics is an "omics" technique that seeks to measure the small organic biomolecules produced by cells (Oliver et al. 1998; Fiehn 2002). Because these small molecules are the end-products of multiple levels of metabolic regulation, their concentrations provide a temporal snapshot of the metabolic state or phenotype of an organism. In particular, metabolites produced by nonenzymatic reactions, such as those formed by reaction with a radical oxygen species, or whose production is regulated by other small molecules, must be monitored directly because their production cannot be inferred from genomic or proteomic information. Metabolomics can be used as a diagnostic tool, identifying biomarkers of disease within the human metabolome, such as cancers (Armitage and Barbas 2014) and Crohn's Disease (Jansson et al. 2009). Metabolomics has also been applied in a wide range of organisms and environments, examining how metabolite abundances respond to environmental factors. In the oceans, marine metabolites have been a valuable source of new natural products, while other metabolomics applications are still rare but growing. For example, recent marine culture experiments have revealed metabolite production not predicted by genomic information (Baran et al. 2010; Fiore et al. 2015), metabolic shifts in response to a specific metabolite (Johnson et al. 2016), and changes in the quantity and composition of metabolite production during coculturing (Paul et al. 2012). Complementary field studies are now underway in several laboratories to understand microbial activity and organic matter cycling in situ. In these studies, metabolomics has great potential to reveal marine microbe phenotypic expression under differing environmental conditions and the chemical interactions by which ecological communities function, as well as the role that these communities play in the marine carbon cycle.

In our laboratory, metabolomics analyses are conducted with complementary untargeted and targeted mass spectrometry techniques (Kido Soule et al. 2015; Longnecker

*Correspondence: winnjohnson@gmail.com

Additional Supporting Information may be found in the online version of this article.

et al. 2015). The targeted method, which is the focus of this study, currently measures 89 metabolites using liquid chromatography tandem mass spectrometry (LC-MS/MS) and an electrospray ionization (ESI) source (Kido Soule et al. 2015). The targeted molecules encompass many classes of metabolites, including amino acids, nucleotides, vitamins, osmolytes, and intermediates of primary metabolism. This paper characterizes the impact of matrix composition (i.e., all of the chemical components of a sample) on both the extraction and analysis of these metabolites.

Metabolomic analysis of seawater samples is challenging due to the complexity of the background organic matter, low concentrations of metabolites, and high levels of salt in the matrix, which may affect instrument response through ionization suppression or enhancement. ESI, in particular, is known to be susceptible to such matrix effects. In complex sample matrices, the coelution of matrix material with the analyte of interest can change the efficiency with which the analyte enters the gas phase relative to the efficiency in pure solvent (King et al. 2000; Taylor 2005; Böttcher et al. 2007). Thus, when using a calibration curve made in pure solvent, the difference in the instrument response factor between the calibration curve and the analyte in the sample matrix can result in inaccurate quantification. For accurate quantification, analytical chemists generally correct for these matrix-specific effects on ionization efficiency by using a standard addition method or a matrix-matched calibration curve with isotopically labeled internal standards (Stüber and Reemtsma 2004; Kang et al. 2007; Boyd et al. 2008). These methods are effective but not always practical. The standard addition method is not feasible when there is a limited amount of sample material available or when a large number of samples must be analyzed. Similarly, isotopically labeled internal standards can be prohibitively expensive, and isotopically labeled metabolites are often not commercially available.

Components of seawater matrices not only affect the mass spectrometer response through ionization suppression or enhancement but the nonvolatile salts can also precipitate, clogging the ESI needle and the mass spectrometer inlet. Working with high-salinity samples thus requires an extraction method that will remove salt. Moreover, dissolved metabolites in marine samples are often dilute and require a method that will successfully concentrate molecules with a wide range of physical and chemical properties. Typically, extractions of organic molecules are optimized for a specific compound class such as amino acids or lipids. In these cases, the structural similarity of the molecules of interest facilitates selection of an extraction method tailored for that functional group, polarity, or charge. For instance, lipids, which are typically hydrophobic or amphiphilic, can be extracted from water using a nonpolar solvent (Cequier-Sánchez et al. 2008), while amino acids can be isolated using a ligand exchange resin (Lee and Bada 1975). However, there are limited options for extracting a structurally diverse array of metabolites using a single technique that can be easily performed in the field.

Solid phase extraction (SPE) has proven to be a straightforward way to extract dissolved organic compounds from seawater with near-complete removal of salt (Lara and Thomas 1994; Dittmar et al. 2008), particularly where large volumes of water must be sampled (we typically extract 4 liters of seawater in the field). In marine organic geochemistry, a commonly used SPE substrate is a modified styrene-divinylbenzene polymer called PPL (Agilent Bond Elut PPL). In the marine environment, this polymer has been shown to have a superior extraction efficiency for marine dissolved organic carbon (DOC; 43–62%) compared to other SPE resins such as C18 and C8 silica-based sorbents (Dittmar et al. 2008). The samples are acidified to pH 2–3 prior to SPE in order to protonate organic acids to improve retention by the sorbent (Dittmar et al. 2008; Longnecker 2015), although protonation of nitrogen-containing compounds may reduce retention of those molecules. This extraction technique has been used to study the composition of low-molecular-weight dissolved organic matter (DOM; < 1000 Da) from samples collected throughout the ocean. Thus, using the PPL SPE polymer for dissolved metabolite extractions allows for more direct comparison with previous studies. The PPL polymer is best suited for extraction of uncharged, slightly polar, medium-sized ($\sim$ 100–1000 Da) analytes. Most charged or very small molecules are not well retained, if at all. However, extraction efficiencies of individual compounds on this polymer cannot be precisely predicted based on molecular structure, highlighting the importance of experimentally determining these parameters.

While PPL SPE is used in a variety of environmental and biomedical applications to extract molecules of interest, studies of extraction efficiency have primarily been confined to a limited set of related molecules without comparison across variable matrix conditions. For example, the extraction efficiencies of acyl homoserine lactones (20–100% recovery) and of drugs such as vancomycin (47% recovery) and furosemide (68% recovery) using PPL SPE have been measured (Li et al. 2006; Baranowska et al. 2010). To our knowledge, there has been no comprehensive study of PPL SPE extraction efficiency for a core set of metabolites. Furthermore, there is currently little information available regarding matrix effects on metabolite quantification in marine samples, thus limiting our ability to predict these effects. For researchers applying targeted metabolomics methods in complex matrices, metabolite extraction efficiencies and matrix effects are essential parameters to incorporate into experimental design and interpretation.

Here we measure the extraction efficiency of 89 dissolved metabolites using SPE and characterize how a range of sample matrices commonly encountered in marine metabolomics affect both extraction efficiency and ESI efficiency of target metabolites. The five matrices selected range from minimal

Table 1. Experimental treatments and their dissolved organic carbon (DOC) concentrations before and after PPL SPE extraction.

Matrix	Milli-Q (MQ)	TIS	VSW	Spent medium from *R. pomeroyi* (Rpom)	Spent medium from *M. pusilla* (Mp)
DOC (μM) before extraction	1	13	107	1865	597
Volume extracted (mL)	1000	1000	1000	250	250
DOC (μM) in extract	200	400	9000	23,000	35,000
DOC bulk extraction efficiency (%)	—	20	51	5	24
Extract volume (mL)	6	6	6	1	1

organic matter to high organic matter concentrations and from salt free to the typical salt content of marine samples. The organic matter composition also varies in the matrices from a higher proportion of recalcitrant organic molecules in seawater compared to spent media treatments where small, polar, labile molecules from cell exudates and lysates will dominate. This allows us not only to examine the matrix effects within common marine sample types but also to consider the impact of specific matrix parameters on analyte behavior within a wider range of metabolomics samples.

Materials and methods

Materials

All metabolite standards were obtained from Sigma-Aldrich at the highest purity available with the following exceptions: dimethylsulfoniopropionate (DMSP), which was purchased from Research Plus; 2,3-dihydroxypropane-1-sulfonate (DHPS) and acetyltaurine, which were donated by Dr. Mary Ann Moran (University of Georgia); and *S*-(1,2-dicarboxyethyl)glutathione, which was purchased from Bachem. All media and artificial seawater components were purchased from Fisher Scientific (American Chemical Society [ACS] certified) with the exception of sodium orthovanadate from Alexis Biochemicals; ethylenediaminetetraacetic acid, manganese chloride tetrahydrate, zinc sulfate heptahydrate (ReagentPlus, $\geq$ 99%), and cobalt chloride hexahydrate (ACS Reagent) from Sigma-Aldrich; and magnesium sulfate heptahydrate (98%), copper sulfate pentahydrate (ACS Reagent), sodium molybdate dihydrate (99+%), selenious acid (99+%), and potassium chromate (99.5%) from Acros Organics. Hydrochloric acid (trace metal grade), acetonitrile (Optima grade), and methanol (Optima grade) were purchased from Fisher Scientific. All water was purified by a Milli-Q system (Millipore; resistivity 18.2 MΩ cm at 25°C, TOC $<$ 1 μM). Glassware was acid washed and combusted in an oven at 460°C for at least 5 h. All plasticware was washed with Citranox and then soaked in a 10% HCl acid bath overnight. Plasticware and media stock solutions were autoclaved before use.

Matrices

Five matrices were tested in this study (Table 1). They will be referred to by the acronyms identified here throughout the rest of the paper. A pure water matrix (MQ) was collected from the Milli-Q system. The artificial seawater matrix (Turks Island Salts [TIS]) was constituted in Milli-Q water as follows (per liter of water): 28 g sodium chloride, 670 mg potassium chloride, 5.5 g magnesium chloride hexahydrate, 6.9 g magnesium sulfate heptahydrate, 1.45 g calcium chloride dehydrate. The seawater matrix (Vineyard Sound Seawater [VSW]) was collected from Vineyard Sound, Massachusetts, and filtered through a 0.2 μm filter (Omnipore [polytetrafluoroethylene], EMD Millipore). The heterotrophic bacterium spent medium matrix (Rpom) consisted of spent medium from a culture of *Ruegeria pomeroyi* sacrificed during the stationary phase of growth and filtered through a 0.2 μm filter (Omnipore, EMD Millipore). Similarly, the autotrophic spent medium matrix (Mp) consisted of spent medium from a culture of *Micromonas pusilla* sacrificed during stationary growth phase and filtered through a 0.1 μm filter (Omnipore, EMD Millipore). See Supporting Information Table S1 for media recipe details.

Sample preparation for extraction efficiency determination

Triplicate bottles (polycarbonate for MQ, TIS, and VSW matrices and glass jars for Rpom and Mp matrices) of each matrix were spiked with a standard mix ($\sim$ 50 : 50 water : methanol) of metabolites of interest (see experimental design in Fig. 1 and Supporting Information Table S2 for volumes and concentrations) and acidified to pH 2–3 with 12 M hydrochloric acid (Dittmar et al. 2008; Longnecker 2015). The spike concentrations were in the nM range to ensure determination of extraction efficiency although many metabolites are measured at pM concentrations in the ocean. An additional triplicate set of bottles without the standard metabolite mix spike was used as a control. The bottles were shaken and allowed to sit for 30 min. Each solution was then loaded onto a methanol-rinsed 1 g Agilent Bond Elut PPL cartridge (6 mL cartridge volume) and the water was pulled through the cartridge using a vacuum pump. The cartridge was rinsed with 24 mL 0.01 M HCl, and the metabolites were eluted with 6 mL methanol (Dittmar et al. 2008). All samples for LC-MS/MS analysis (control and standard mix extracts) were dried down in a vacufuge and reconstituted in 95 : 5 water : acetonitrile (see Supporting Information Table S2 for volumes; 1% of the final volume was 5 μg

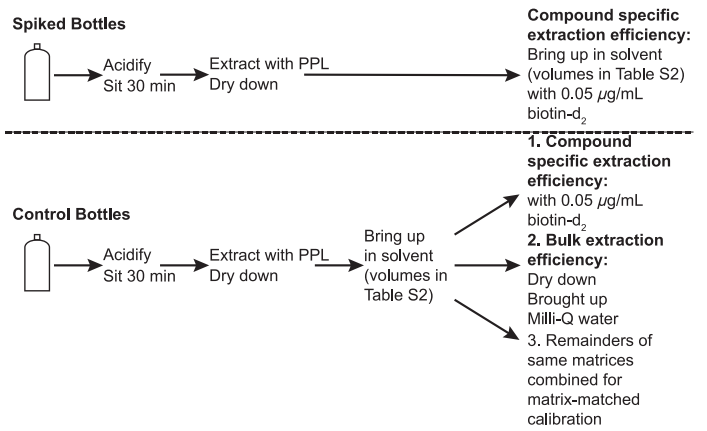

Fig. 1. Experimental design. For the spiked samples (top), all of the extract was prepared for LC-MS analysis. However, for the control samples (bottom), some of the extract was needed to determine the extraction efficiency for each matrix and to make the matrix-matched calibration curves as well as to perform the LC-MS analysis. Thus, the extract was divided into three parts so that it could be used for all of these purposes.

mL^{-1} biotin-d_2 as an injection standard). An aliquot of the control extract (without biotin-d_2) was used to make matrix-matched calibration curves for each matrix treatment and to determine the bulk organic carbon extraction efficiency of the PPL cartridge (see below; Fig. 1). The matrix-matched calibration curves contained nine calibration points ranging from 0.5 ng mL^{-1} to 1000 ng mL^{-1}. Further discussion of how the calibration curves were made can be found in Supporting Information Table S3, Text S1, and Fig. S1.

Determination of limits of detection

Data from nine calibration curves made in Milli-Q water collected over 6 months (April–September 2015) were used to calculate a limit of detection (LOD). This is defined as (Boyd et al. 2008):

$$\text{LOD} = \text{stdA} \times t \text{ value}$$

where stdA is the standard deviation of the concentration of the analyte at a selected low concentration and t value refers to the Student's t-test interval for a one-tailed t-test with $\alpha = 0.01$ and $n - 1$ degrees of freedom. For the majority of metabolites, the 1 ng mL^{-1} calibration point was used to calculate the standard deviation. However, in some cases a higher concentration had to be used. This method requires that the concentration used to calculate the LOD be 1–5 times higher than the calculated LOD. The LOD was calculated at multiple low concentrations for each metabolite to determine the most appropriate concentration for providing an accurate LOD (Supporting Information Table S4). Outliers were identified using a Generalized Extreme Studentized Deviate Test and up to two outliers were excluded from the calculation. The limit of quantification (LOQ) was calculated with respect to the LOD by using the definition (Boyd et al. 2008):

$$\text{LOQ} = \frac{10}{3} \times \text{LOD}$$

The LOD and LOQ in the other matrices could not be calculated directly due to the presence of analytes in the matrix itself. Instead, we used the ratio of the analyte signal in a given matrix to the analyte signal in MQ to adjust the LOD and LOQ calculated in MQ, according to the following calculation:

$$\text{eLOD}_i \textit{ or } \text{eLOQ}_i = \frac{\text{LOD}_{\text{mq}} \text{ or } \text{LOQ}_{\text{mq}}}{\frac{\left(\overline{A_{\text{t}}} - \overline{A_{\text{b}}}\right)_i}{\overline{A_{\text{mq}}}}}$$

where eLOD_i is the estimated LOD in matrix i, eLOQ_i is the estimated LOQ in matrix i, LOD_{mq} is the LOD calculated in MQ, LOQ_{mq} is the LOQ calculated in MQ, A_{t} is the total response of the analyte at 5 ng mL^{-1} (or 50 ng mL^{-1} if no peak intensity at 5 ng mL^{-1}) in matrix i, A_{b} is the background analyte response (no spiked standard) in matrix i, and A_{mq} is the response of the analyte in MQ at the same concentration. All of these measurements were made in quadruplicate. This type of ratio has been proposed to evaluate matrix effects (Rogatsky and Stein 2005) although it has not been used to estimate LOD values to our knowledge. eLOD_i and eLOQ_i values were only calculated for the VSW and Rpom matrices.

Organic carbon measurements

The total organic carbon concentrations of the samples were measured before and after the PPL extraction. Prior to extraction, 40 mL water samples of each matrix type (in triplicate) were acidified to pH 2–3 using 12 M hydrochloric acid. To determine the amount of organic carbon retained on the PPL cartridge, the remaining PPL-extracted control sample (not spiked with metabolite standard mix, as described above) was dried down in the vacufuge and brought up in 1 mL of Milli-Q water. Four hundred milliliter of that 1 mL was added to a vial of 25 mL Milli-Q water and 25 μL of 12 M hydrochloric acid. Samples were stored at 4°C until analysis. All samples were analyzed using a Shimadzu TOC-V_{CSH} Total Organic Carbon Analyzer, according to standard practices. A five-point calibration curve made with potassium hydrogen phthalate was used and blanks were run regularly. Duplicate injections had an average coefficient of variability of $< 1\%$. Comparisons to standards from D. Hansell (University of Miami) were made daily.

Mass spectrometry

LC-MS/MS analysis was performed on a Phenomenex C18 reversed phase column (Synergi Fusion, 2.1 × 150 mm, 4

μm) coupled via a heated ESI source to a triple quadrupole mass spectrometer (Thermo Scientific TSQ Vantage) operated under selected reaction monitoring mode (SRM) with polarity switching (Kido Soule et al. 2015). Quantification and confirmation SRM transitions were monitored for each metabolite. Eluent A was Milli-Q water with 0.1% (v/v) formic acid and Eluent B was acetonitrile with 0.1% (v/v) formic acid. The following gradient was used: hold at 5% B for 2 min; ramp to 65% B for 16 min; ramp to 100% B for 7 min and hold for 8 min. An 8.5-min column re-equilibration with the starting ratio of eluents was carried out between sample analyses. Between the different matrices, a Milli-Q water blank and three samples of unspiked matrix extract were run to rinse and condition the column. Composite chromatograms of a sample from each matrix type are shown as examples in the supplemental information (Supporting Information Fig. S2).

Data processing

XCalibur RAW files from the mass spectrometer were converted to mzML files using MSConvert (Chambers et al. 2012). MAVEN (Melamud et al. 2010; Clasquin et al. 2012) was used to select and integrate peaks. Peaks below a MAVEN quality threshold of 0.4 (on a scale of 0–1) were discarded. To enhance confidence in metabolite identification, quantification and confirmation peaks were required to have retention times within 12 s (0.2 min) of each other. Future data processing of environmental samples should include a peak quality control check for the confirmation ion, but this is not necessary when working with commercial standards. Calibration curves were required to have at least five calibration points and points were selected to range from the lowest concentration level to one concentration level above the highest concentration detected in an experimental sample (Supporting Information Table S5). To compare the response factors (slopes) between matrices, the full calibration curve up to 1000 ng mL^{-1} was used. Spiked metabolite concentrations were calculated directly from calibration curves without subtracting metabolite concentrations in matrix controls because the calibration curves were matrix matched and so already incorporated any necessary correction for the background concentration of the metabolite. Extraction efficiencies of individual metabolites were calculated using the following formula:

$$\%EE = \frac{CF_i}{CT_i} \times 100$$

where %EE is the percent extraction efficiency, CF_i is the final concentration of the analyte measured in ng mL^{-1}, and CT_i was the target concentration of the analyte assuming 100% retention (either 500 ng mL^{-1} or 1500 ng mL^{-1}, see Supporting Information Tables S2, S7).

Structural characterization

To link the extraction efficiency of analytes to their structure, their structural characteristics were assessed in a number of ways. SPARC (http://archemcalc.com/), an online computational tool, was used to calculate the charge and partitioning coefficients of metabolites based on their structure. Specifically, these calculations were carried out at pH 2, as this was at the extreme end of the pH range used during SPE, and accounted for the ionic strength of seawater. K_{oc} (the partitioning coefficient between water and generic organic carbon) was calculated for metabolites that were well retained on the PPL cartridges to examine whether metabolites that had improved extraction efficiencies in the culture matrices had similar water-organic carbon partitioning coefficients. The partitioning coefficient for hexadecane and water was also calculated for metabolites to determine if it had a relationship with the measured extraction efficiencies. These data are not included as no relationship was found. Other information such as polar surface area and molecular weight were obtained from the online chemical database ChemSpider; but yielded no relationship with extraction efficiency for our metabolites.

Assessment

Matrix characterization

The five matrices used in this study were chosen to examine how organic matter concentration and type, as well as salt, influence analyte behavior during extraction and instrument analysis. In particular, we compared minimal-organic matter and salt-free matrices to common matrices encountered in marine metabolomics samples. These include field samples from the ocean and spent seawater media from controlled laboratory experiments. We measured the organic carbon content of each matrix before and after SPE to have a quantitative measure of the carbon-based differences between the selected matrices (Table 1). The MQ treatment provides a salt- and organic matter-free (1 μM) baseline comparison. Similarly, in order to separately examine the effect of salt, TIS contains minimal organic matter (13 μM) but has the same salt concentration as seawater. The rest of the matrix treatments were a range of sample types containing both salt and organic matter. The VSW matrix had a dissolved organic carbon content of 107 μM, and a large portion is recalcitrant and relatively non-polar (compared to the culture matrices) due to its low heteroatom (oxygen and nitrogen) content (reviewed by Carlson and Hansell 2015; Repeta 2015).

The organic carbon measurements before and after PPL extraction were used to determine a bulk dissolved organic carbon (DOC) extraction efficiency for each of the matrices. The DOC extraction efficiency in the VSW matrix was higher (51%) than either of the spent media matrix samples (Table 1). In contrast, the bulk DOC extraction efficiency in the

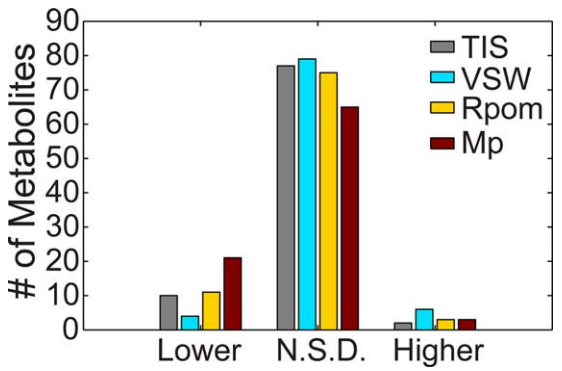

Fig. 2. The number of metabolites with a lower, higher, or not significantly different (N.S.D.) instrument response factor in each matrix relative to the MQ matrix. The *p*-value was considered significant if $p < 0.05$.

Rpom matrix was poor (5%). The high initial DOC concentration (1865 μM) is due to the addition of propionate (initial carbon concentration from propionate in the media was 3000 μM) as an organic carbon substrate to fuel the growth of *R. pomeroyi*. Since this molecule is small and highly polar, it is not retained by PPL SPE. The Mp matrix did not contain an added carbon substrate and so the initial DOC pool (597 μM) is primarily composed of cellular exudates and lysates, which explains the higher extraction efficiency (24%). Due to the variable bulk extraction efficiencies of organic carbon, the relative differences in organic carbon concentration were muted in the extracts relative to the initial matrices (final organic carbon contents in the 6 mL [1 mL for spent media] extracts: 9 mM [VSW], 23 mM [Rpom], 35 mM [Mp]).

Instrument response factors

The impact of these matrices on the ionization efficiency of each metabolite in our targeted metabolomics method can be characterized by comparing the instrument response factor (i.e., the slope of the calibration curve) in each matrix to that in MQ (Fig. 2; Supporting Information Table S6). To compare the linear regressions of the analyte calibration curves in TIS, VSW, Rpom, and Mp with those of the analytes in MQ, we used a wild bootstrap method (Estévez-Pérez et al. 2016), which generated the *p*-values reported in Supporting Information Table S6. Calibration curve slopes for an analyte were considered significantly different between a matrix and MQ when *p*-values were less than 0.05 (Fig. 2). Estévez-Pérez et al. (2016) found this random resampling approach to be the most consistent way to compare linear calibration curves in cases such as this, where there are relatively few calibration points and the data are not homoscedastic.

In general, more metabolites exhibit ionization suppression in the spent media matrices (Rpom and Mp) compared to TIS and VSW (Fig. 2). This appears to be linked to the total DOC content of the matrices as the Rpom and Mp extracts contained 23 mM and 35 mM DOC, respectively (excluding the spiked metabolites). In contrast, the TIS and VSW extracts contained lower concentrations of 0.4 mM and 9 mM DOC, respectively. However, it is possible that differences in organic matter composition between the matrices also play a role. When the distribution of instrument response factor ratios in each matrix is compared, there is a significant difference between the distributions in the two media matrices compared to those of the non-culture matrices (Supporting Information Fig. S3). Therefore, as we would predict, increased matrix DOC content affects the ionization efficiency of some metabolites; but this impact is not statistically significant for most metabolites on an individual basis. Even in the most extreme case (Mp), 73% of metabolites were unaffected.

There are 10, 4, 11, and 21 metabolites in the TIS, VSW, Rpom, and Mp matrices, respectively, that have response factors that are lower than in MQ and 2, 6, 3, and 3 metabolites with response factors that are higher than in MQ, all with *p*-values below 0.05 (Fig. 2). The affected metabolites elute from the column at a wide range of retention times and vary between the matrices, making it difficult to predict which metabolites will be affected. Some metabolites are relatively consistent across matrices; putrescine, for instance, which elutes from the column early, has a significantly elevated response factor in three of the four matrices, while cyanocobalamin, with a relatively late retention time, has a significantly decreased response factor in all four matrices. Taurocholic acid, with a retention time of 17 min, is only significantly reduced in the Mp matrix, while malic acid, with a retention time of 1.9 min, has decreased ionization efficiencies in both Rpom and Mp. These are notable observations because not only do these metabolites have different polarities and functional groups, but they are also ionized in distinct matrix environments due to their different retention times. These results suggest that changes in response factor are linked to DOC content but are also molecule specific. However, for the purpose of method implementation, when the majority of metabolites are considered, the effect of the matrix on instrument response at the measured DOC concentrations is not significant and thus does not require a matrix-matched calibration approach. Rather, standard curves in Milli-Q water provide good quantification (within a factor of 2) for most metabolites in this study.

Extraction efficiency

Extraction efficiencies for targeted metabolites by PPL SPE were determined in the five matrices (Supporting Information Table S7). As shown in Fig. 3, there is a general consensus across all matrices between LC retention time and extraction efficiency; metabolites with later retention times are better retained on the PPL cartridge. For example, in the VSW and Rpom matrices, consistent SPE retention of all analytes is not reached until $\sim$ 2.5 min in the chromatogram

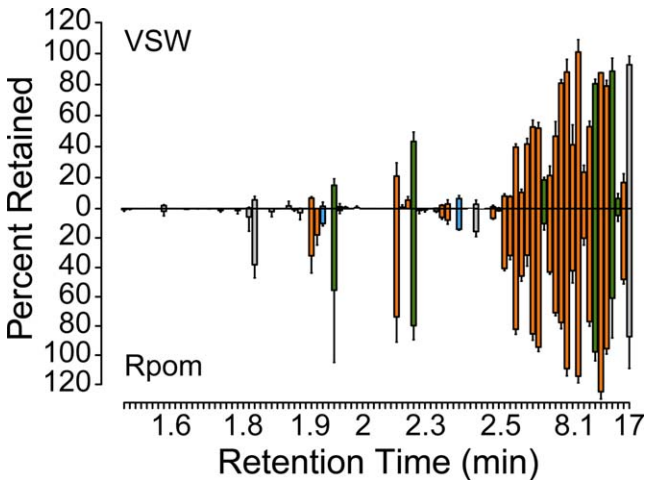

Fig. 3. The extraction efficiency for each metabolite plotted by retention time (not scaled) for the VSW and Rpom matrices. Orange bars indicate compounds with aromatic functional groups, green bars are compounds that are neutrally charged at pH 2 but not aromatic, blue are nonaromatic compounds whose charge could not be determined, and gray bars are compounds that are charged at pH 2 or have an extremely polar functional group like phosphate.

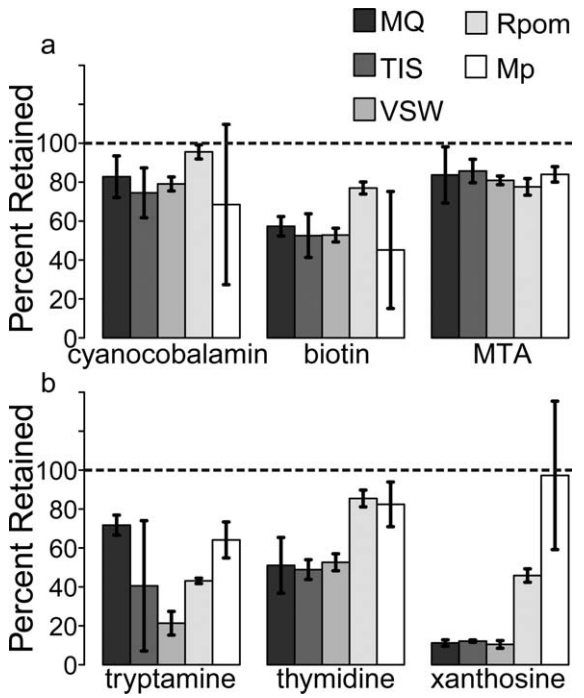

Fig. 4. Comparison of extraction efficiencies of select metabolites across all five matrices. (**a**) Examples of metabolites that are consistently retained in all matrices. MTA: 5-methylthioadenosine. (**b**) Examples of metabolites that are variably retained in different matrices (tryptamine) or have enhanced extraction efficiencies in the spent media matrices (thymidine and xanthosine).

(Fig. 3). However, the extraction efficiencies of a few metabolites run contrary to this general trend. The extraction efficiency for *S*-(5′-adenosyl)-L-homocysteine (SAH) is greater than 10% but its column retention time is less than 2.5 min. Conversely, a small group of metabolites have column retention times greater than 2.5 min but have extraction efficiencies less than 10%: xanthine, inosine 5′-monophosphate (IMP), inosine, guanosine, *N*-acetylglutamic acid, and desthiobiotin.

The structural attributes that distinguish metabolites that are retained on the PPL resin from those that are not seem to be a combination of aromaticity, charge at pH 2, and secondarily molecular weight (Fig. 3; Supporting Information Table S8). Overall, aromatic compounds or those that are neutral at pH 2 seem to be best retained. For example, SAH's predominant species is positively charged (a small fraction is amphiphilic) at pH 2, but it is an aromatic compound and retained by the PPL resin. However, other aromatic compounds are not well retained by PPL, and size and charge may be factors in these cases. For example, xanthine is quite small, as it is a purine nucleobase and lacks a sugar functional group. In contrast, inosine and guanosine contain a sugar moiety but their positive charge may offset the size benefit of the sugar. IMP contains a phosphate group, which may make it too polar to be retained, despite its aromaticity. Other metabolites, such as *N*-acetylglutamic acid and desthiobiotin, are neutral at pH 2, but are small and not aromatic, perhaps leading to their poor retention. A partitioning coefficient that shows a relationship with the measured extraction efficiencies could not be identified, despite our efforts. For example, the partitioning coefficient (log D) for hexadecane and water does not systematically explain the extraction efficiencies. While there are structural differences that appear to govern metabolite retention on the SPE polymer, the variable impacts of aromaticity, charge, and molecular size preclude straightforward prediction of retention dynamics at this time.

In addition to metabolite chemical and physical properties, the sample matrix can affect metabolite extraction efficiency (Fig. 4). In particular, of the 35 metabolites that were retained on the PPL cartridge, 14 had higher extraction efficiencies in the culture matrices (Rpom and Mp; see Supporting Information Table S7) than in the other three matrices (MQ, TIS, and VSW). For instance, thymidine and xanthosine both show improved extraction efficiency in the culture matrices (Fig. 4b). We hypothesize that colloidal organic matter in the culture matrices could be trapped on the polymer and provide additional sites for the metabolites to interact. Although we could determine a structural trend for metabolites that are best retained on the PPL, similar probing of structural patterns of metabolites that showed improved extraction efficiency in the culture matrices did not yield any clear relationship. Characteristics such as aromaticity, charge, molecular weight, log K_{oc} (pH 2), and polar surface area of metabolites were examined (Supporting Information Table S9) without uncovering a clear relationship.

Table 2. Instrumental limits of detection (LOD) and limits of quantification (LOQ) in MQ, estimated (eLOD) for the VSW and Rpom matrices,* and limits of detection for field samples†,‡ (— indicates cases where the LOD could not be calculated due to high variability in the data, and n.r. indicates metabolites that are not retained on the PPL polymer).

Compound	LOD (ng mL^{-1})	LOQ (ng mL^{-1})	VSW eLOD (ng mL^{-1})	Rpom eLOD (ng mL^{-1})	LOD in Seawater 100% EE (pM)†	LOD in Seawater PPL EE (pM)‡
(6R)-5,6,7,8-Tetrahydrobiopterin	—	—	—	—	—	—
1-Deoxy-D-xylulose-5-phosphate	7.4	25	12 ± 2	27 ± 18	6.9 ± 1.2	n.r.
2,3-Dihydroxybenzoic acid	8.3	28	6.4 ± 0.4	6.8 ± 0.5	5.2 ± 0.4	33 ± 3
DHPS	5.9	20	29 ± 72	36 ± 150	23 ± 58	n.r.
3-Mercaptopropionic acid	11	38	12 ± 2	10 ± 3	12 ± 2	78 ± 15
4-Aminobenzoic acid	0.63	2.1	0.65 ± 0.03	0.69 ± 0.04	0.59 ± 0.03	7.9 ± 1.9
4-Hydroxybenzoic acid	17	58	16 ± 3	18 ± 4	15 ± 2	95 ± 16
5-Methylthioadenosine	0.80	2.7	0.67 ± 0.04	0.59 ± 0.18	0.28 ± 0.02	2.0 ± 0.4
6-Phosphogluconic acid	44	150	48 ± 42	110 ± 140	22 ± 19	n.r.
Acetyltaurine	7.5	25	9 ± 3	26 ± 10	6.6 ± 2.0	n.r.
Adenine	1.9	6.3	2.2 ± 0.6	7 ± 9	2.0 ± 0.6	n.r.
Adenosine	1.5	5.0	1.4 ± 0.2	2.0 ± 0.4	0.68 ± 0.11	120 ± 23
Adenosine 5′-monophosphate	2.4	7.9	17 ± 34	10 ± 0.9	6 ± 12	n.r.
Alpha-ketoglutaric acid	5.8	19	39 ± 190	16 ± 13	33 ± 170	n.r.
Arginine	2.3	7.7	7 ± 4	7 ± 5	5 ± 3	n.r.
Aspartic acid	—	—	—	—	—	—
Betaine	2.9	9.7	3.9 ± 0.7	4.2 ± 0.5	4.2 ± 0.7	n.r.
Biotin	2.3	7.5	1.5 ± 0.2	1.5 ± 0.2	0.76 ± 0.11	8.0 ± 1.3
Caffeine	0.18	0.58	0.15 ± 0.03	0.15 ± 0.03	0.10 ± 0.02	2.5 ± 0.5
Chitobiose	5.7	19	5 ± 6	11 ± 16	1.5 ± 1.8	n.r.
Chitotriose	20	66	13 ± 3	49 ± 40	2.5 ± 0.5	n.r.
Choline	1.9	6.2	1.7 ± 0.2	2.2 ± 0.4	2.1 ± 0.3	n.r.
Ciliatine	2.5	8.2	3.3 ± 09	3.4 ± 0.6	3.3 ± 0.9	n.r.
Citric acid	41	140	24 ± 9	22 ± 6	15 ± 6	n.r.
Citrulline	2.0	6.5	2.7 ± 0.8	6 ± 2	1.9 ± 0.6	n.r.
Cyanocobalamin	2.1	6.9	1.2 ± 0.3	1.3 ± 0.6	0.11 ± 0.02	0.8 ± 0.2
Cysteine	8.5	28	11 ± 2	29 ± 10	12 ± 2	n.r.
Cytosine	2.3	7.6	1.9 ± 1.4	2.7 ± 1.8	2.2 ± 1.5	n.r.
D-(-)3-Phosphoglyceric acid	24	81	10 ± 11	58 ± 125	7 ± 7	n.r.
D-Glucosamine 6-phosphate	3.7	12	5.1 ± 1.6	0.58 ± 0.05	2.5 ± 0.8	n.r.
D-Ribose 5-phosphate	5.2	17	7.1 ± 9.8	12 ± 13	4 ± 5	n.r.
Desthiobiotin	0.75	2.5	0.56 ± 0.04	0.2 ± 0.5	0.33 ± 0.03	25 ± 16
Dihydroxyacetone phosphate	4.9	16	1 ± 3	6 ± 12	1.1 ± 1.8	n.r.
DMSP	0.99	3.3	1.2 ± 0.1	2.0 ± 0.2	1.1 ± 0.1	n.r.
Ectoine	0.85	2.8	0.75 ± 0.09	0.71 ± 0.10	0.66 ± 0.08	n.r.
Folic acid	0.57	1.9	0.35 ± 0.08	0.33 ± 0.08	0.10 ± 0.02	0.7 ± 0.3
Fosfomycin	27	89	59 ± 19	—	53 ± 17	n.r.
Fumaric acid	—	—	—	—	—	—
GABA	1.4	4.8	1.3 ± 0.3	2.0 ± 0.4	1.5 ± 0.3	n.r.
Glucose 6-phosphate	8.9	30	13 ± 2	64 ± 87	6.2 ± 0.8	n.r.
Glutamic acid	36	120	19 ± 10	45 ± 36	17 ± 9	n.r.
Glutamine	0.86	2.9	1.3 ± 0.2	1.6 ± 0.4	1.1 ± 0.2	n.r.
Glutathione	5.1	17	7 ± 9	80 ± 32	3 ± 4	n.r.
Glutathione oxidized	15	50	5 ± 6	42 ± 98	1.0 ± 1.3	n.r.
Glyphosate	5.1	17	3 ± 5	15 ± 26	2 ± 3	n.r.
Guanine	2.1	6.9	1.8 ± 0.3	14 ± 10	1.5 ± 0.3	n.r.

TABLE 2. Continued

Compound	LOD (ng mL^{-1})	LOQ (ng mL^{-1})	VSW eLOD (ng mL^{-1})	Rpom eLOD (ng mL^{-1})	LOD in Seawater 100% EE (pM)[†]	LOD in Seawater PPL EE (pM)[‡]
Guanosine	0.44	1.5	0.39 ± 0.10	0.46 ± 0.12	0.17 ± 0.05	17 ± 5
Indole 3-acetic acid	1.1	3.7	1.1 ± 0.1	1.1 ± 0.1	0.77 ± 0.08	7.0 ± 0.8
Inosine	2.0	6.8	2.4 ± 0.7	3.3 ± 1.6	1.1 ± 0.3	76 ± 30
IMP	9.4	31	5.7 ± 1.0	8 ± 2	1.8 ± 0.3	n.r.
(Iso)Leucine	4.0	13	4 ± 3	2.5 ± 1.7	4 ± 3	n.r.
Kynurenine	1.6	5.3	1.3 ± 0.2	1.6 ± 0.2	0.79 ± 0.13	8.3 ± 1.9
Malic acid	26	85	27 ± 22	30 ± 22	26 ± 21	n.r.
Methionine	4.8	16	48 ± 17	58 ± 25	40 ± 14	n.r.
Muramic acid	—	—	—	—	—	—
N-acetylglucosamine	16	54	16 ± 4	76 ± 62	9 ± 2	n.r.
N-acetylglutamic acid	5.5	18	6 ± 15	7 ± 4	4 ± 10	2400 ± 6000
N-acetylmuramic acid	21	70	18 ± 4	17 ± 4	7.8 ± 1.9	1500 ± 1300
NAD	—	—	—	—	—	—
NADP	49	160	16 ± 19	28 ± 33	3 ± 3	n.r.
Ornithine	3.1	10	6 ± 4	12 ± 19	5 ± 4	n.r.
Orotic acid	30	100	27 ± 8	53 ± 19	22 ± 7	n.r.
Pantothenic acid	15	51	12 ± 1	12 ± 1	6.7 ± 0.6	80 ± 15
Phenylalanine	0.67	2.2	0.73 ± 0.11	0.3 ± 0.2	0.56 ± 0.09	15 ± 3
Phosphoenolpyruvate	—	—	—	—	—	—
Proline	2.1	6.9	2.0 ± 0.5	3.7 ± 1.2	2.2 ± 0.5	n.r.
Putrescine	31	100	39 ± 7	46 ± 14	55 ± 10	n.r.
Pyridoxine	1.4	4.5	1.4 ± 0.3	1.2 ± 0.2	1.1 ± 0.2	240 ± 45
Riboflavin	0.63	2.1	0.35 ± 0.04	0.3 ± 0.2	0.12 ± 0.02	0.65 ± 0.08
S-(1,2-dicarboxyethyl)glutathione	4.1	14	1.4 ± 1.9	2 ± 3	0.4 ± 0.6	n.r.
SAH	1.9	6.3	4 ± 4	18 ± 68	1.4 ± 1.2	72 ± 64
S-Adenosyl methionine	7.6	25	6.2 ± 1.9	5.0 ± 1.7	1.9 ± 0.6	n.r.
Sarcosine	23	75	34 ± 13	42 ± 15	48 ± 19	n.r.
Serine	1.8	6.0	2.9 ± 0.9	3.6 ± 1.8	3.5 ± 1.0	n.r.
sn-Glycerol 3-phosphate	9.6	32	9 ± 8	21 ± 22	7 ± 6	n.r.
Succinic acid	—	—	—	—	—	—
Taurine	3.4	11	0.4 ± 0.4	0.5 ± 0.5	0.4 ± 0.4	n.r.
Taurocholic acid	5.3	18	2.3 ± 0.8	2.5 ± 0.8	0.57 ± 0.20	5 ± 2
Thiamin	39	130	36 ± 5	19 ± 3	17 ± 2	n.r.
Thiamin monophosphate	21	69	18 ± 3	18 ± 3	6.1 ± 1.0	n.r.
Threonine	1.7	5.8	2.5 ± 1.2	2.8 ± 1.0	2.6 ± 1.2	n.r.
Thymidine	19	64	20 ± 7	21 ± 6	10 ± 3	120 ± 52
Tryptamine	0.43	1.4	0.42 ± 0.03	0.45 ± 0.03	0.32 ± 0.02	2.7 ± 0.3
Tryptophan	5.3	18	6.1 ± 0.8	5.5 ± 0.4	3.7 ± 0.5	30 ± 5
Tyrosine	3.2	11	3.3 ± 1.4	8 ± 18	2.3 ± 0.9	1100 ± 550
Uracil	4.4	15	5 ± 4	—	6 ± 4	n.r.
Uridine 5′-monophosphate	40	130	—	—	—	—
Xanthine	2.0	6.8	1.8 ± 0.7	2.2 ± 0.4	1.5 ± 0.5	n.r.
Xanthosine	2.1	6.9	2.0 ± 0.4	2.0 ± 0.7	0.88 ± 0.17	47 ± 11

GABA, γ-aminobutyric acid.

*LOD and LOQ were calculated in Milli-Q water as described in the Experimental Section. The estimated (eLOD) values for the VSW and Rpom matrices were adjusted from the LOD values as described in the Experimental Section.

[†]These values were calculated to reflect the LOD (using the VSW eLOD) in the initial seawater sample assuming that 100% of the analyte was extracted from 4 L of water and that the final extract was 500 μL.

[‡]This LOD represents the lowest value we would expect to detect in a field sample given the PPL SPE extraction efficiencies determined here and our current sampling protocol; 4 L of seawater is extracted, then eluted with 6 mL of methanol, dried down, and reconstituted in 3 mL 95 : 5 water : acetonitrile. This was calculated only for metabolites with at least a 1% extraction efficiency.

The extraction efficiencies reported here will serve as a useful guide to researchers intending to extract metabolites using PPL SPE from samples with similar organic carbon content. To our knowledge, this study is the most extensive look at the extraction efficiencies for a core set of metabolites using SPE. However, the variability in extraction efficiency across matrix types indicates that care must be taken when extrapolating these values to other sample matrices.

Limits of detection and quantification

The instrument LOD provides a conservative estimate of the concentration at which a metabolite can be confidently detected, but not reliably quantified. In contrast, the instrument LOQ is defined to be a higher (more conservative) level where we expect reliable quantification. LOD and LOQ were calculated for all metabolites in Milli-Q water using the EPA definitions (Table 2; Glaser et al. 1981; EPA 1997; Boyd et al. 2008). This definition of the LOD ensures with 99% confidence that the analyte is greater than zero; however, there is a 50% chance of a false negative because any measurement that falls on the low side of a normal distribution will be below the limit. LOD values range from 0.2 ng mL^{-1} for caffeine to 49 ng mL^{-1} for nicotinamide adenine dinucleotide phosphate (NADP). As a general rule metabolites with early retention times have higher LODs due to increased baseline noise in the early part of the chromatogram. Polyamines (putrescine, ornithine) and metabolites with phosphate groups, in particular, often have low quality peaks that are difficult to integrate at low concentrations.

Discussion

This study examined analyte behavior at a number of points in the process of sample preparation and analysis for a targeted metabolomics method. Ultimately, the efficiency of these processes limits the concentrations of metabolites we can measure in the ocean and in cultures. Due to the presence of the analytes in the non-MQ matrices, the LOD and LOQ could not be calculated directly for those matrices, but were instead estimated (eLOD: Table 2; eLOQ: Supporting Information Table S4) to account for ion enhancement or suppression in each matrix. The eLODs for many metabolites in the VSW and Rpom matrices are similar to the calculated LOD in MQ, however, there seem to be more metabolites with elevated eLODs and greater uncertainty in the Rpom matrix compared to the VSW matrix (Table 2).

In Table 2, the lowest concentrations we can expect to measure in the ocean for a given metabolite using our sampling method are reported, based on the adjusted eLOD for VSW. Both the total concentration that could be measured assuming 100% extraction efficiency and the concentration that can be measured accounting for the PPL SPE extraction efficiency in VSW are calculated. While this paper has focused on extraction of dissolved metabolites, we have previously determined $\sim$ 100% extraction efficiency for particulate or intracellular metabolites (Kido Soule et al. 2015). For the dissolved metabolites, concentrations range from <1 pM to $\sim$ 2000 pM (or $\sim$ 2 nM). The highest detection limits are constrained by extremely low SPE extraction efficiencies. Of course, if the focus is an individual metabolite that is poorly retained on PPL, another extraction method should be found. Nonetheless these values suggest that our method can measure low concentrations of many metabolites in the field, an essential capability in the marine environment. For example, riboflavin, a B vitamin, has been measured at concentrations of 0.5–7 pM in the ocean (Sañudo-Wilhelmy et al. 2012). Accounting for riboflavin's extraction efficiency and eLOD in VSW, our detection limit in the ocean is 0.6 pM, allowing us to adequately detect typical concentrations in the ocean. Concentrations of phenylalanine around 1.5 nM have been measured in estuarine environments (Coffin 1989), which is well above the calculated detection limit of 15 pM for our method. This targeted metabolomics method will allow us to undertake the task of mapping the oceanic distributions and concentrations of these molecules, many of which have never been measured in the ocean.

Conclusions

The impact of solution matrix composition on the extraction efficiency and instrument response factor of the analytes was unexpected. The extraction efficiency differed significantly depending on the organic matter content of the matrix, with 40% of the metabolites retained by the polymer having enhanced extraction efficiencies in the culture matrices compared to MQ, TIS, and VSW. Higher matrix DOC concentrations were also linked to increased ionization suppression and enhancement relative to MQ, but only for a minority of analytes, with 11% of metabolites having a significantly different response factor in VSW compared to 27% in Mp. This trend might be exacerbated at even higher matrix DOC concentrations than those studied here.

This dataset provides practical information that can be used to back-calculate estimates of initial analyte concentrations and also characterizes the impact of a number of representative marine matrices. For those working in marine or aquatic systems, the PPL SPE extraction efficiency trends observed should be particularly useful, as they will allow researchers to anticipate whether an analyte is likely to be observed using this method, and also further informs our understanding of the structural selectivity of this extraction method which may be relevant to past and future studies that characterize DOM extracted with this polymer. While the gold standard for absolute metabolite quantification within a complex matrix remains the standard addition method, these results suggest that, in the cases analyzed here, the matrix does not compromise quantification.

References

Armitage, E. G., and C. Barbas. 2014. Metabolomics in cancer biomarker discovery: Current trends and future perspectives. J. Pharm. Biomed. Anal. **87**: 1–11. doi:10.1016/j.jpba.2013.08.041

Baran, R., B. P. Bowen, N. J. Bouskill, E. L. Brodie, S. M. Yannone, and T. R. Northen. 2010. Metabolite identification in *Synechococcus* sp. PCC 7002 using untargeted stable isotope assisted metabolite profiling. Anal. Chem. **82**: 9034–9042. doi:10.1021/ac1020112

Baranowska, I., A. Wilczek, and J. Baranowski. 2010. Rapid UHPLC method for simultaneous determination of vancomycin, terbinafine, spironolactone, furosemide and their metabolites: Application to human plasma and urine. Anal. Sci. **26**: 755–759. doi:10.2116/analsci.26.755

Böttcher, C., E. Roepenack-Lahaye, E. Willscher, D. Scheel, and S. Clemens. 2007. Evaluation of matrix effects in metabolite profiling based on capillary liquid chromatography electrospray ionization quadrupole time-of-flight mass spectrometry. Anal. Chem. **79**: 1507–1513. doi:10.1021/ac061037q

Boyd, R. K., C. Basic, and R. A. Bethem. 2008. Trace quantitative analysis by mass spectrometry, John Wiley & Sons.

Carlson, C. A., and D. A. Hansell. 2015. DOM sources, sinks, reactivity, and budgets, p. 65–102. *In* D. A. Hansell and C. A. Carlson [eds.], Biogeochemistry of marine dissolved organic matter. Elsevier.

Cequier-Sánchez, E., C. Rodríguez, Á. G. Ravelo, and R. Zárate. 2008. Dichloromethane as a solvent for lipid extraction and assessment of lipid classes and fatty acids from samples of different natures. J. Agric. Food Chem. **56**: 4297–4303. doi:10.1021/jf073471e

Chambers, M. C., and others. 2012. A cross-platform toolkit for mass spectrometry and proteomics. Nat. Biotechnol. **30**: 918–920. doi:10.1038/nbt.2377

Clasquin, M. F., E. Melamud, and J. D. Rabinowitz. 2012. LC-MS data processing with MAVEN: A metabolomic analysis and visualization engine. Curr. Protoc. Bioinforma. **37**: 1–23. doi:10.1002/0471250953.bi1411s37

Coffin, R. B. 1989. Bacterial uptake of dissolved free and combined amino acids in estuarine waters. Limnol. Oceanogr. **34**: 531–542. doi:10.4319/lo.1989.34.3.0531

Dittmar, T., B. Koch, N. Hertkorn, and G. Kattner. 2008. A simple and efficient method for the solid-phase extraction of dissolved organic matter (SPE-DOM) from seawater. Limnol. Oceanogr.: Methods. **6**: 230–235. doi:10.4319/lom.2008.6.230

EPA. 1997. Guidelines establishing test procedures for the analysis of pollutants (App. B, Part 136, Definition and procedures for determination of the method detection limit). U.S. Code of Federal Regulations, Title 40.

Estévez-Pérez, G., J. M. Andrade, and R. R. Wilcox. 2016. Bootstrap approach to compare the slopes of two calibrations when few standards are available. Anal. Chem. **88**: 2289–2295. doi:10.1021/acs.analchem.5b04004

Fiehn, O. 2002. Metabolomics–the link between genotypes and phenotypes. Plant Mol. Biol. **48**: 155–171. doi:10.1023/A:1013713905833

Fiore, C. L., K. Longnecker, M. C. Kido Soule, and E. B. Kujawinski. 2015. Release of ecologically relevant metabolites by the cyanobacterium, *Synechococcus elongatus* CCMP 1631. Environ. Microbiol. **17**: 3949–3963. doi:10.1111/1462-2920.12899

Glaser, J. A., D. L. Foerst, G. D. McKee, S. A. Quave, and W. L. Budde. 1981. Trace analyses for wastewaters. Environ. Sci. Technol. **15**: 1426–1435. doi:10.1021/es00094a002

Jansson, J., B. Willing, M. Lucio, A. Fekete, J. Dicksved, J. Halfvarson, C. Tysk, and P. Schmitt-Kopplin. 2009. Metabolomics reveals metabolic biomarkers of Crohn's disease. PLoS One. **4**: e6386. doi:10.1371/journal.pone.0006386

Johnson, W. M., M. C. Kido Soule, and E. B. Kujawinski. 2016. Evidence for quorum sensing and differential metabolite production by the marine bacterium in response to DMSP. ISME J. **10**: 2304–2316. doi:10.1038/ismej.2016.6

Kang, J., L. A. Hick, and W. E. Price. 2007. Using calibration approaches to compensate for remaining matrix effects in quantitative liquid chromatography/electrospray ionization multistage mass spectrometric analysis of phytoestrogens in aqueous environmental samples. Rapid Commun. Mass Spectrom. **21**: 4065–4072. doi:10.1002/rcm

Kido Soule, M. C., K. Longnecker, W. M. Johnson, and E. B. Kujawinski. 2015. Environmental metabolomics: Analytical strategies. Mar. Chem. **177**: 374–387. doi:10.1016/j.marchem.2015.06.029

King, R., R. Bonfiglio, C. Fernandez-Metzler, C. Miller-Stein, and T. Olah. 2000. Mechanistic investigation of ionization suppression in electrospray ionization. J. Am. Soc. Mass Spectrom. **11**: 942–950. doi:10.1016/S1044-0305(00)00163-X

Lara, R. J., and D. N. Thomas. 1994. Isolation of marine dissolved organic matter: Evaluation of sequential combinations of XAD resins 2, 4, and 7. Anal. Chem. **66**: 2417–2419. doi:10.1021/ac00086a032

Lee, C., and J. L. Bada. 1975. Amino acids in equatorial Pacific Ocean water. Earth Planet. Sci. Lett. **26**: 61–68. doi:10.1016/0012-821X(75)90177-6

Li, X., and others. 2006. Development and application of a method for the analysis of N-acylhomoserine lactones by solid-phase extraction and ultra high pressure liquid chromatography. J. Chromatogr. A. **1134**: 186–193. doi:10.1016/j.chroma.2006.09.047

Longnecker, K. 2015. Dissolved organic matter in newly formed sea ice and surface seawater. Geochim. Cosmochim. Acta. **171**: 39–49. doi:10.1016/j.gca.2015.08.014

Longnecker, K., J. Futrelle, E. Coburn, M. C. Kido Soule, and E. B. Kujawinski. 2015. Environmental metabolomics: Databases and tools for data analysis. Mar. Chem. **177**: 366–373. doi:10.1016/j.marchem.2015.06.012

Melamud, E., L. Vastag, and J. D. Rabinowitz. 2010. Metabolomic analysis and visualization engine for LC-MS data. Anal. Chem. **82**: 9818–9826. doi:10.1021/ac1021166

Oliver, S. G., M. K. Winson, D. B. Kell, and F. Baganz. 1998. Systematic functional analysis of the yeast genome. Trends Biotechnol. **16**: 373–378. doi:10.1016/S0167-7799(98)01214-1

Paul, C., M. A. Mausz, and G. Pohnert. 2012. A co-culturing/metabolomics approach to investigate chemically mediated interactions of planktonic organisms reveals influence of bacteria on diatom metabolism. Metabolomics **9**: 349–359. doi:10.1007/s11306-012-0453-1

Repeta, D. J. 2015. Chemical characterization and cycling of dissolved organic matter, p. 41–47. *In* D. A. Hansell and C. A. Carlson [eds.], Biogeochemistry of marine dissolved organic matter. Elsevier.

Rogatsky, E., and D. Stein. 2005. Evaluation of matrix effect and chromatography efficiency: New parameters for validation of method development. J. Am. Soc. Mass Spectrom. **16**: 1757–1759. doi:10.1016/j.jasms.2005.07.012

Sañudo-Wilhelmy, S. A., and others. 2012. Multiple B-vitamin depletion in large areas of the coastal ocean. Proc. Natl. Acad. Sci. USA. **109**: 14041–14045. doi:10.1073/pnas.1208755109

Stüber, M., and T. Reemtsma. 2004. Evaluation of three calibration methods to compensate matrix effects in environmental analysis with LC-ESI-MS. Anal. Bioanal. Chem. **378**: 910–916. doi:10.1007/s00216-003-2442-8

Taylor, P. J. 2005. Matrix effects: The Achilles heel of quantitative high-performance liquid chromatography-electrospray-tandem mass spectrometry. Clin. Biochem. **38**: 328–334. doi:10.1016/j.clinbiochem.2004.11.007

Acknowledgments

Support for W.M.J. came from a National Defense Science and Engineering Fellowship. The authors would also like to thank the following people for their assistance with experimental design, lab work, and data analysis and interpretation: Krista Longnecker, Cara Fiore, Yina Liu, David Griffith, and Philip Gschwend. This work was funded by the Gordon and Betty Moore Foundation (grant 3304 to E.B.K.) and the National Science Foundation (grant OCE-1154320 to E.B.K and K.L.). Funding is also gratefully acknowledged from Simons Foundation International. The instruments in the WHOI FT-MS Facility were purchased with support from the GBMF and NSF.

Conflict of Interest

None declared.

Submitted 03 November 2016
Revised 01 February 2017
Accepted 19 February 2017

Associate editor: Paul Kemp